Advances in Science and Technology Research Journal

Advances in Science and Technology Research Journal 2023, 17(5), 248–259
https://doi.org/10.12913/22998624/172565
ISSN 2299-8624, License CC-BY 4.0

Received: 2023.08.28
Accepted: 2023.09.19
Published: 2023.10.20

Numerical Study of the Effect of the Trailing-Edge Devices (Gurney Flap and Divergent Trailing-Edge Flap) on the Aerodynamic Characteristics of an Airfoil in Transonic Flow for Drone Applications

Małgorzata Kmiotek[1*], Adrian Kordos[1], Adam Piszczatowski[2], Adam Zaremba[2]

[1] Department of Aerospace Engineering, Faculty of Mechanical Engineering and Aeronautics Rzeszow University of Technology, Al. Powstańców Warszawy 12, 35-959 Rzeszów, Poland

[2] Student from Faculty of Mechanical Engineering and Aeronautics Rzeszow University of Technology, Al. Powstańców Warszawy 12, 35-959 Rzeszów, Poland

* Corresponding author's e-mail: kmimal@prz.edu.pl

ABSTRACT

The primary objective of this research was to examine how the inclusion of mini Trailing-edge devices (referred to as mini TEDs) impacts the aerodynamic properties of the RAE-2822 airfoil. Utilizing ANSYS Fluent software, we conducted numerical simulations to analyze the behavior of compressible flow around the airfoil, specifically at a Mach number (Ma) of 0.73, while varying the angles of attack. The mini TEDs employed in our simulations comprised a Gurney flap and a divergent trailing-edge. Our findings demonstrate that incorporating these mini TEDs at the trailing-edge leads to a noteworthy increase in the lift coefficient (CL) and drag coefficient (CD). However, it is worth noting that this enhancement resulted in an improved lift-to-drag ratio for the airfoil for specific angles of attack. These outcomes underscore the potential advantages of employing mini TEDs to enhance aerodynamic performance, especially in aerospace drone applications.

Keywords: trailing-edge devices, gurney flap, divergent trailing-edge flap, transonic flow, drone.

INTRODUCTION

Enhancing aerodynamic characteristics through the use of devices is a dynamic area of research within applied aerodynamics [1, 2]. Among the most widely adopted devices for improving aerodynamic performance are Trailing-Edge Devices affixed to the rear edge of surfaces [3]. One such device is the flap, a Trailing-Edge Device primarily employed to augment the aerodynamic efficiency of wings during flight. Among the myriad flap variations, miniature Trailing-edge devices (abbreviated as mini TEDs) hold particular fascination among researchers [4, 5]. Miniature Trailing-edge devices encompass an array of flow control mechanisms positioned at the Trailing-edge of airfoils. In comparison to conventional control surfaces, mini TEDs are notably diminutive. While conventional Trailing-edge flaps typically occupy 10% to 30% of the local wing chord, mini TEDs generally are constrained to a size of 2% or less of the wing chord. These mini TEDs encompass various flap types, such as the Gurney flap, Divergent Trailing-edge (DTE) flap, and split flap, as depicted in Figure 1.

The Gurney flap (GF) is a perpendicular flap attached to the underside of the profile at the Trailing-edge, characterized by a geometric parameter denoting its height (h_{GF}). The Divergent Trailing-edge flap signifies a modification to the Trailing-edge, defined by two geometric parameters: length (l_{DTE}) and height (h_{DTE}). Meanwhile, the split flap, a hinged flap situated anterior to the Trailing-edge, is described by three parameters: the location of the split-flap hinge (x_{SF}), the length of the split-flap (l_{SF}), and the deflection angle of the split-flap (δ_{SF}). The Gurney flap was initially employed in motor racing, with driver Dan

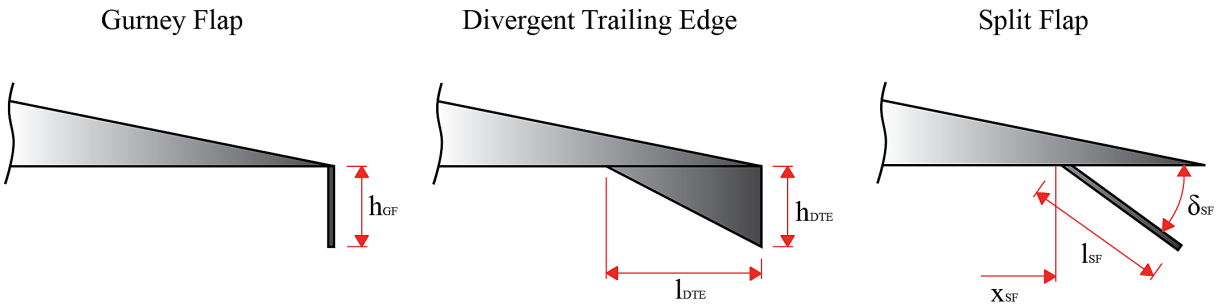

Fig. 1. Miniature trailing-edge devices (mini TEDs) [13]

Gurney pioneering its application. He was the first to affix a straight flap atop his car's spoiler, designed to enhance tire grip during acceleration and cornering [6]. The Gurney flap has found promising applications in wind turbine blades [7] and shows high potential for drones at low Reynolds numbers [8]. The Gurney flap has found utility in transonic flight, sparking interest in its impact on wing aerodynamics, primarily centered around augmenting lift generation. This increase in lift translates to shorter runway requirements and improved payload capacity. Furthermore, an elevated lift-to-drag coefficient ratio offers numerous ancillary benefits, including reduced fuel consumption and enhanced aircraft range.

Robert H. Leibeck [9] conducted experimental research to explore the effects of a simple flap on boosting lift for the Newman profile at subsonic speeds. His observations revealed that lift increased while drag decreased for specific angles of attack. He posited that, for optimal aerodynamic performance, the Gurney flap's ideal height typically falls within 1 to 2% of the wing's chord length. Despite advancements in geometrical profile optimization techniques [10], there remains room for enhancing the aerodynamic performance of transonic profiles by merely modifying the Trailing-edge—altering its direction or introducing alternative solutions [11]. Computational simulations conducted by B.E. Thompson and R.D. Lotz [12] demonstrated that employing the Divergent Trailing-edge (DTE) flap resulted in a rearward shift of the boundary layer separation point along the top edge of the profile, thereby improving efficiency.

Nonetheless, the Gurney flap exerts a more pronounced influence on profile performance than the Divergent Trailing-edge (DTE) flap, offering a more straightforward solution that doesn't necessitate fundamental profile shape alterations. Y.C. Li conducted experimental investigations into the Gurney flap and the Divergent Trailing-edge flap's impact on airfoil aerodynamics, as presented in [11]. The findings indicated that, in contrast to the DTE flap, the Gurney flap wielded a more significant influence on lift and aerodynamic efficiency.

T. Yu et al. explored the effect of Gurney flap height variations on the RAE-2822 profile using numerical analysis, encompassing subsonic and transonic speeds across different angles of attack at specific Mach numbers [13]. Generally, they observed that increased Gurney flap height resulted in elevated lift production. However, the highest maximum lift-to-drag ratio was attained at a flap height of 0.25% of the chord length.

The primary application of the Gurney flap at subsonic speeds involves recuperating lost lift. For instance, a variable leading edge slope (VDLE) profile was introduced in helicopters to manage dynamic stalls and associated adverse pitch moment alterations. This, however, came at a cost of a 10% lift loss. The Gurney flap was affixed to regain lost lift at the Trailing-edge. Chandrasekhar [14] noted that, due to significant changes in rotor blade angles of attack, optimizing the Gurney flap's height was imperative, with a height of 1% chord length deemed most effective. Maughmer [15] pointed out that the detrimental increase in drag induced by the Gurney flap is primarily linked to its height; larger sizes progressively elevate drag. Several studies have sought to optimize the Gurney flap's size, revealing that its effective height typically falls between 1% and 2% of the chord length. Giguere and other researchers [16] indicated that the optimal lift-to-drag force ratio occurs when the Gurney flap's height aligns with the boundary layer thickness. Yachen Li et al. [17] conducted experimental research on the NACA 0012 profile at a Reynolds number of $2 \cdot 10^6$, shedding light on how the Gurney flap's location and attachment angle

influence its effectiveness. In all attachment configurations, they observed increased lift and drag forces. Optimal performance was achieved when the Gurney flap was set at a 45-degree angle, with the highest lift force occurring at a 90-degree angle. Mounting the flap at the Trailing-edge yielded the best performance.

In [18], the authors presented test results for miniature Trailing-edge devices, including the Gurney flap, Divergent Trailing-edge flap, and split flap. Experimental and numerical assessments were conducted on the VC-Opt (Variable Camber Optimized) profile at a Reynolds number of $5 \cdot 10^6$, spanning rake angles from -3° to 5°. These studies demonstrated that all tested mini TED types functioned by effectively altering the airfoil's angle of attack and redistributing pressure over the rear portion. For a fixed angle of attack, lift and drag increased while the heeling moment decreased. Mini TEDs significantly influenced supersonic conditions in transonic flight, particularly impacting lift and drag characteristics. At medium and high lift coefficients, drag reduction was attainable, yielding an improved lift-to-drag ratio compared to the baseline profile. Reductions in overall transonic flow resistance were primarily due to the mini TEDs' wave resistance offsetting their resistance. Exploring the influence of geometric parameter modifications, it was found that changes in Gurney flap height and split flap attachment angle δ_{SF} yielded similar effects. However, the split flap's impact was less pronounced at the same mini TED effective height. The Divergent Trailing-edge flap displayed analogous aerodynamic characteristics to the split flap.

In the literature, numerous studies investigate the impact of mini TEDs on aircraft aerodynamics for both subsonic and transonic flows [19] [20, 21]. Given the expanding use of unmanned aerial vehicles (UAVs) and their diverse applications, particularly in the realm of transonic drones [22, 23, 24], there exists substantial potential for enhancing lift generation. As UAV development trends favor compact dimensions and maximum payload capacity, the need for devices to boost lift becomes increasingly evident. Additionally, with the proliferation of electric aviation, there is a growing impetus to develop highly efficient structures. Utilizing mini TED flaps presents an opportunity to enhance the aerodynamic properties of such structures, motivating the research outlined in this article.

Different aircraft types, designed for specific purposes like long-distance travel, agriculture, or search and rescue missions, require distinct internal structures. Strength, weight, and reliability are the primary considerations in aircraft structures, dictating the requirements for materials used in construction and repair [25]. Reliability is crucial to minimize the risk of unexpected failures. Aircraft structures experience various stresses, including tension, compression, shear, bending, and torsion, which are absorbed by different wing components and transmitted to the fuselage. Wings play a significant role in generating lift to elevate an aircraft, and they must maintain their aerodynamic shape under extreme stresses. Therefore, when designing mini TEDs, material properties should be considered. The choice of materials significantly influences the quality and reliability of aircraft structures, which are pivotal for progress in the aviation industry. Aircraft structures demand lightweight, mechanically resilient, and corrosion-resistant materials [26].

This work aims to analyze the impact of elements affixed to the Trailing-edge of mini Trailing-Edge Devices, specifically the Gurney flap and the Divergent Trailing-edge flap, on the aerodynamic characteristics of the RAE2822 profile, with potential applications in transonic drones. Numerical simulations were executed using the finite volume method, constructing a two-dimensional airfoil model with mini TED devices – the Gurney flap and the Divergent Trailing-edge flap. These simulations, conducted through the ANSYS Fluent program, facilitated the examination of how these flaps and their geometric dimensions influence aerodynamic force coefficients and streamline distributions, shedding light on their impact on transonic drone aerodynamics.

PROBLEM STATEMENT

Numerical method and governing equation

When analyzing flow using Computational Fluid Dynamics (CFD) methods, it is essential to determine the nature of the flow through the appropriate functions implemented in the computational program. The classical Reynolds-Averaged Navier-Stokes equations are based on the assumption of incompressible flow, where density is treated as constant. In the case of steady flow, pressure changes associated with velocities close to the

speed of sound lead to density variations, and the compressibility effects must be considered. When studying turbulent motion, the Reynolds hypothesis is commonly used, which describes turbulent flow as a superposition of averaged and fluctuating flow components. For compressible flow, equations governing the conservation of mass, momentum, and energy must be solved. By substituting defined quantities into the Navier-Stokes equations and the equation of state for compressible fluid flow and performing mass averaging operations, in accordance with [27, 28], we obtain the following conservation equations in form:

- Principles of mass conservation [27, 28]:

$$\frac{\partial \rho}{\partial t} + \mathrm{div}(\rho \bar{V}) = 0 \tag{1}$$

- Principles of conservation of momentum [27], [28]:

$$\rho \frac{\partial \overline{\mathrm{V}}}{\partial \mathrm{t}} = \rho \bar{F} - \mathrm{grad}\, p + \mu \Delta \bar{V} \tag{2}$$

where: $\bar{V}\ \left[\frac{m}{s}\right]$ – velocity vector, $\rho\ \left[\frac{kg}{m^3}\right]$ – fluid density, $\bar{F}\ [N]$ – vector of mass forces, $p\ [Pa]$ – fluid pressure.

- The Reynolds number was determined from the formula:

$$Re = \frac{\rho V_{in} c}{\mu} \tag{3}$$

where: c[m] – chord, $\mu\ \left[\frac{kg}{m \cdot s}\right]$ – dynamic viscosity, $V\ \left[\frac{m}{s}\right]$ – flow velocity.

The Mach number was determined from the formula:

$$M = \frac{V_{in}}{a} \tag{4}$$

where: $a\ \left[\frac{m}{s}\right]$ – the speed of sound.

The 2D simulations were conducted utilizing Computational Fluid Dynamics software, which solves the equations governing continuity, momentum, and energy using the Reynolds-Averaged Navier-Stokes methodology. For this particular investigation, the $k - \omega$ shear stress transport (SST) turbulence model was employed [29].

Computational domain and grid

The airfoil selected for these simulations was the RAE-2822. The analysis incorporated two flaps: the Gurney flap and the Divergent Trailing-edge flap. These flaps were affixed directly onto the Trailing-edge of the airfoil. The specific geometries of these flaps are depicted in Figure 2, while Table 1 provides detailed information regarding their geometric parameters. The flow geometry is presented in Figure 3. The computational domain comprised two parts: semi-circular with a radius equal to 10c and the square of a side 20c to show the complex flow phenomena. The dimensions of the computational domain are presented in Table 2. A structural C-grid was used in the simulations presented, and the total number of mesh elements amounted to an average of 360,000 elements, of which 1,200 are located on the airfoil surface. An example of the mesh used is shown in Figure 4.

Boundary conditions and numerical procedure

The flow was assumed to be two-dimensional, compressible, and steady. The airfoil chord was a characteristic dimension for the Reynolds number. The fluid was an ideal gas (fluid density ρ = 1.0226 kg/m^3, dynamic viscosity was calculated from the Sutherland law and was set to μ = 1.88309·10^{-5} Pa·s). The boundary conditions adopted for the analysis were as follows:

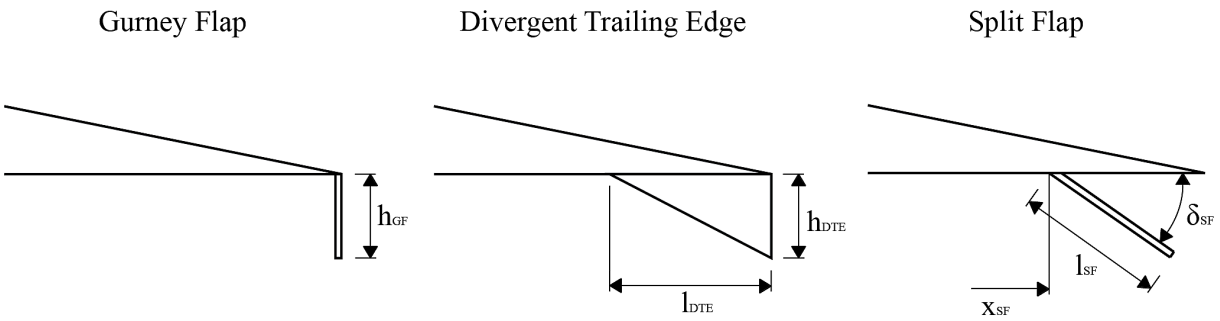

Fig. 2. Geometric parameters of miniature Trailing-Edge Devices

Table 1. Configurations of the geometry flaps

No	Type	Height h_{GF} (h_{DTE})/c [%]	Length l_{DTE}/c [%]
1	Clean	-	-
2	GF	0,5	-
3		1	-
4		1,5	-
5		2	-
6		2,5	-
7		3	-
8	DTE_4	0,5	2
9		1	4
10		1,5	6
11		2	8
12	DTE_6	0,5	3
13		1	6
14		1,5	9
15		2	12

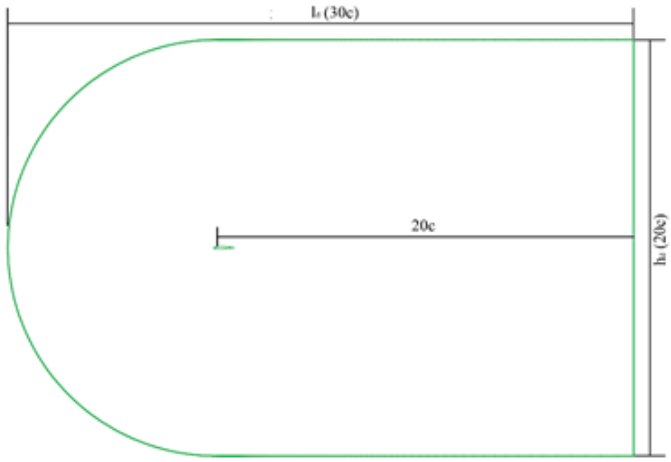

Fig. 3. Computational domain

- Pressure-far-field boundary condition was implemented to establish the behavior of fluid pressure at the outer edges of the computational domain.
- No-slip condition ($\vec{u} = 0$) was enforced to describe the absence of relative motion between the fluid and solid surfaces, ensuring that fluid velocity was zero along the profile.

In this study, the k-ω SST turbulence model was applied, as it showed promising results for both steady and unsteady conditions. The simulation was conducted using the Implicit method, and discretization settings were set to Second Order Upwind for all parameters. The Residuals were discretized to values smaller than 10^{-6} for all equations to achieve high-precision solutions in line with convergence criteria. The ANSYS Fluent 2021 R1 package was used as the solver for conducting compressible flow research. The numerical procedures were as follows:

1. The Density-Based solver type and the Viscous heating option were selected for steady conditions.
2. The Ideal Gas model was chosen for air density changes, and the Sutherland Model was used for dynamic viscosity changes.
3. A value of 0 Pa was set as the Operating Pressure.
4. Simulations were initiated by specifying Mach number and angle of attack parameters.

Additionally, we integrated pressure and static temperature values, obtained from the experimental parameters within the aerodynamic tunnel (gauge pressure = 90410 Pa, temperature = 308 K).

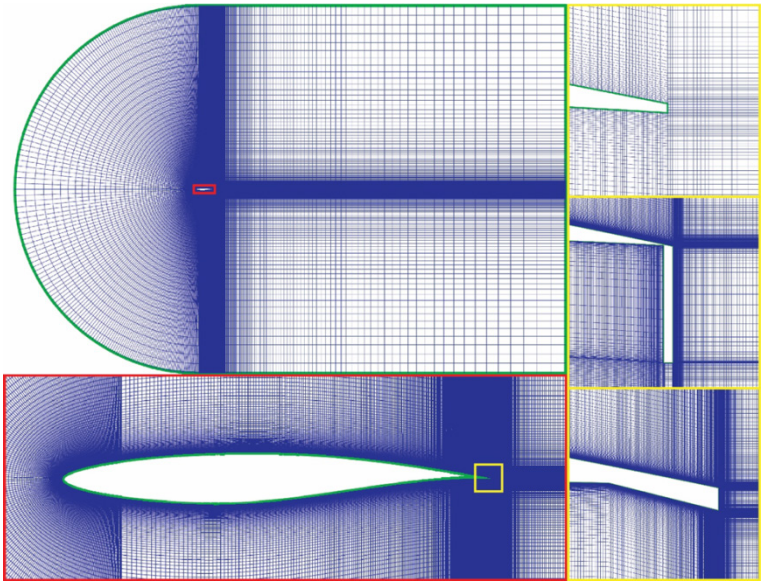

Fig. 4. An example of the computational domain and mesh distribution of airfoils

These values were meticulously selected to align with the requisite Reynolds number, which is calculated based on the profile chord, as elaborated in reference [30].

Validation of the numerical model

To validate the adopted methodology, the simulation results for the RAE-2822 profile for M = 0.731, AOA = 2.81° i Re = 6.5·10^6 were compared with the results of the AGARD report [30]. To compare the numerical results with the experimental results obtained in the wind tunnel, corrections were made, and the influence of the walls was taken into account. The correction method given in [31] was used, considering the measurement tolerance of the control experiment presented in the AGARD report. Table 3 compares the coefficients of aerodynamic forces of the experimental (AGARD) and numerical data. Figure 5 displays the pressure coefficient distribution for the experimental flow and the numerical model, considering the utilization of the k-ω SST turbulence model, both with and without the impact of nearby walls. The comparison of

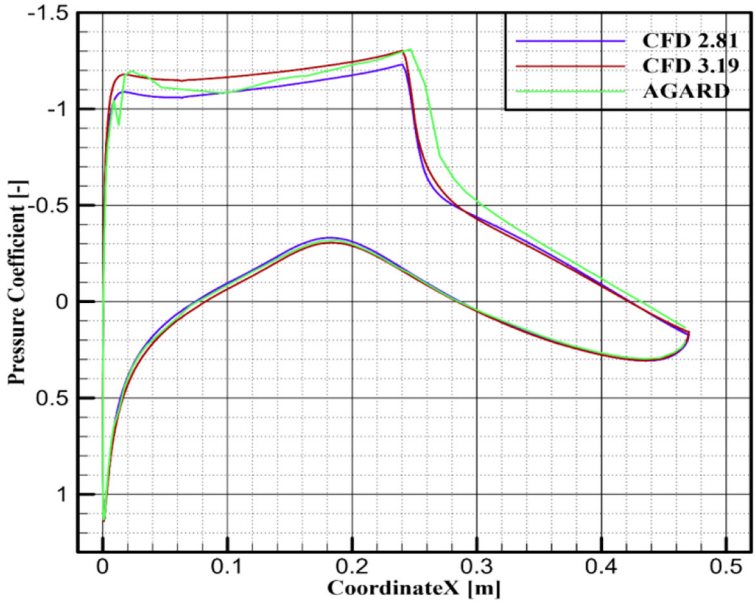

Fig. 5 Airfoil pressure distribution by CFD simulation (with and without wall effect compensation) compared to the experimental results of the airfoil at Re = 6.5·10 ^{6}

Table 2. Parameters used in the calculations

Characteristic	Symbol	Value	Unit
Chord	c	0.47	m
Length	l_d	30 c	m
Height	h_d	20 c	m
Inlet velocity	V_{in}	257.08	m/s
The speed of sound	a	352.17	m/s

Table 3. Comparison of research results of the AGARD report with the conducted numerical study (CFD)

Characteristic	C_L	ΔC_L	C_D	ΔC_D	L/D	Δ(L/D)
AGARD alpha = 3.19°; M=0.730	0.803	-	0.0168	-	47.79	-
CFD, alpha = 2.81°; M=0.731 (wall effect compensation)	0.7385	8.03%	0.01738	3.45%	42.49	11.09%

these results reveals a favorable alignment between the simulation outcomes and the reference data. Consequently, this numerical investigation's credibility is currently under confirmation.

RESULTS AND DISCUSSION

In this study, we examined how the geometric parameters of both the Gurney flap and the Divergent Trailing-edge flap impact the aerodynamic characteristics of a transonic drone wing. This investigation encompassed various angles of attack spanning from -4 to 10 degrees.

Effect of changing the angle of attack on aerodynamic characteristics

Based on our simulations, we determined the aerodynamic coefficients for various geometric configurations of the Gurney flap and the Divergent Trailing-edge flap at different angles of attack. These coefficients include the lift coefficient (C_L) and the drag coefficient (C_D). We presented the collected data graphically in Figures 6 to 10. In these simulations, we maintained a Mach number of M=0.73 and a Reynolds number based on the airfoil's chord length of $Re = 6.5 \cdot 10^6$.

The data are categorized as follows: "CC" denotes clean airfoil curves, "GF X%" represents airfoils with Gurney flap heights of X%, and "DTE X%" corresponds to airfoils with Divergent Trailing-edge flaps of X% height. We also considered two variants of the Divergent Trailing-edge flap, distinguished by the ratio of flap length (l_{DTE}) to flap height (h_{DTE}),

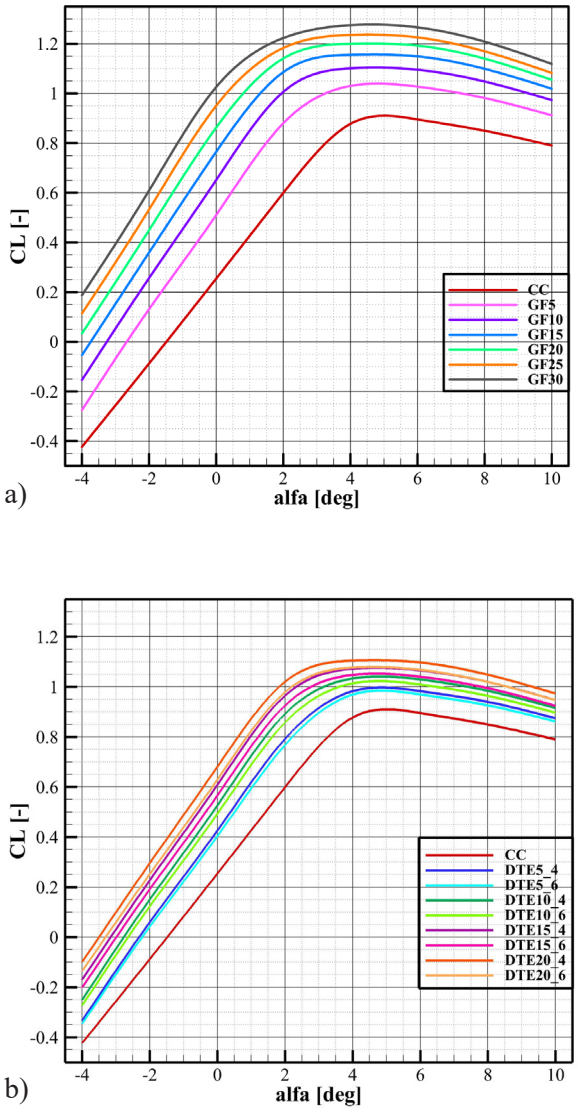

Fig. 6. Comparison of lift coefficients versus alpha of RAE-2822 airfoil (a) with/without GF, (b) with/without DTE.

with ratios of 4 and 6. Figure 6 illustrates the lift coefficient distribution concerning the angle of attack for various flap geometries (GF and DTE) compared to the clean airfoil profile. The results indicate an increase in lift force for each flap type compared to the clean profile. At an angle of attack of 0°, the C_L coefficient increased 1.43 times for the GF_20 flap compared to the DTE_20_4 flap and 1.62 times compared to the DTE_20_6 flap in relation to the clean profile. Notably, the Trailing-edge divergence angle for the Divergent Trailing-edge flap had a discernible effect on lift increase. Comparing the two variants with ratios 4 and 6, an increase in the angle resulted in a 1.14-fold lift enhancement. This lift coefficient increase was consistent across all tested angles of attack. Furthermore, the angle at which zero lift was achieved decreased for both flap configurations compared to the clean profile, with the difference increasing as the flap size increased. This implies that using flaps generated a similar amount of lift at a lower angle of attack, potentially reducing the overall drone's angle of attack and, consequently, drag. Figure 7 presents the drag coefficient distribution concerning the angle of attack for both the clean airfoil profile and profiles with flaps. The data in the graph suggest that flaps increased drag for positive angles of attack while reducing drag for negative angles of attack.

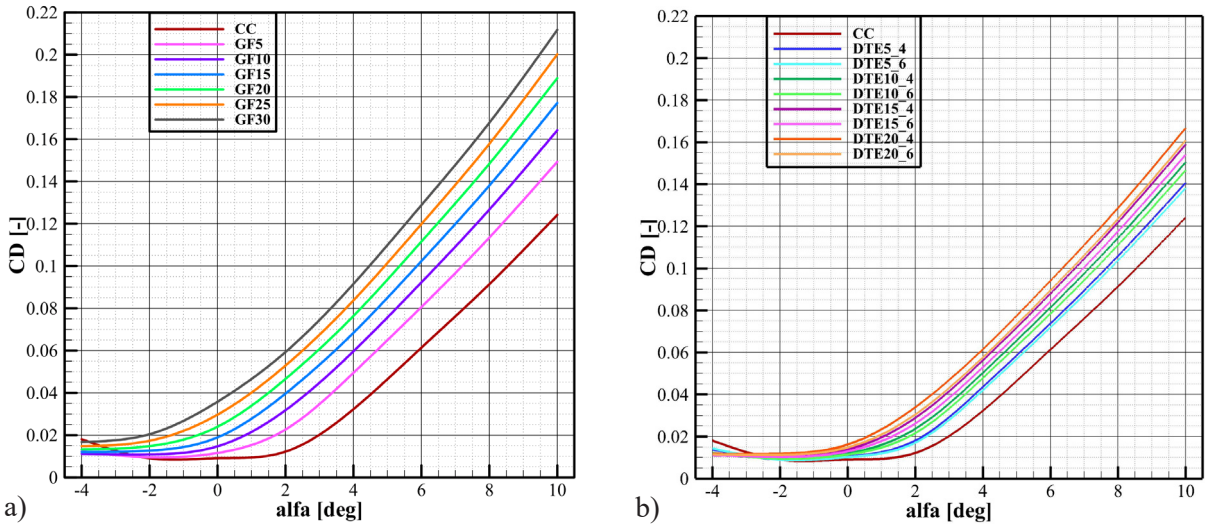

Fig. 7. Comparison of drag coefficients of RAE-2822 airfoil (a) with/without GF, (b) with/without DTE

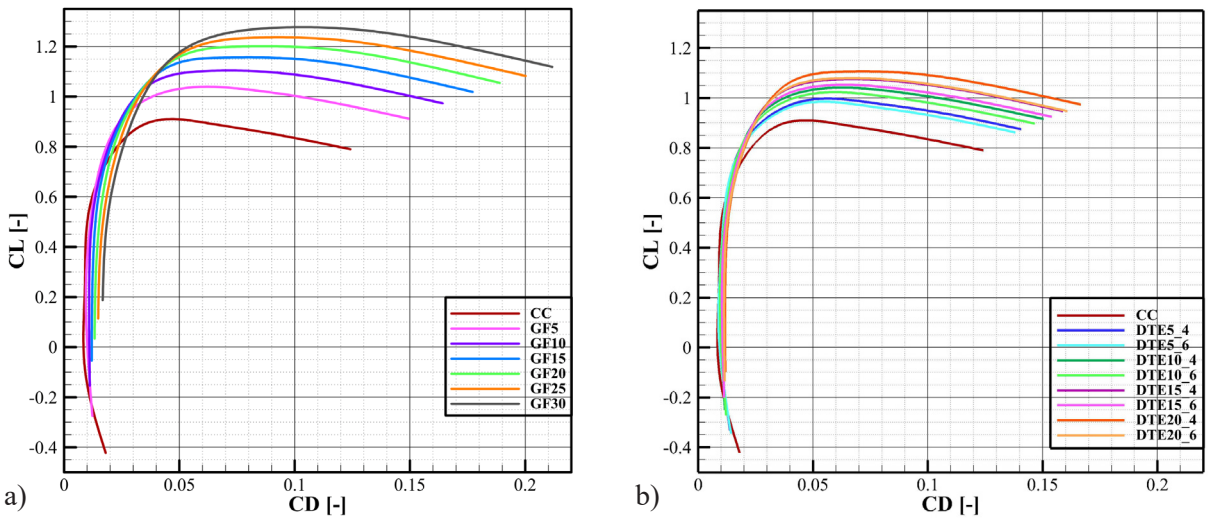

Fig. 8. Comparison of lift coefficients versus drag coefficients of RAE-2822 airfoil (a) with/without GF, b) with/without DTE

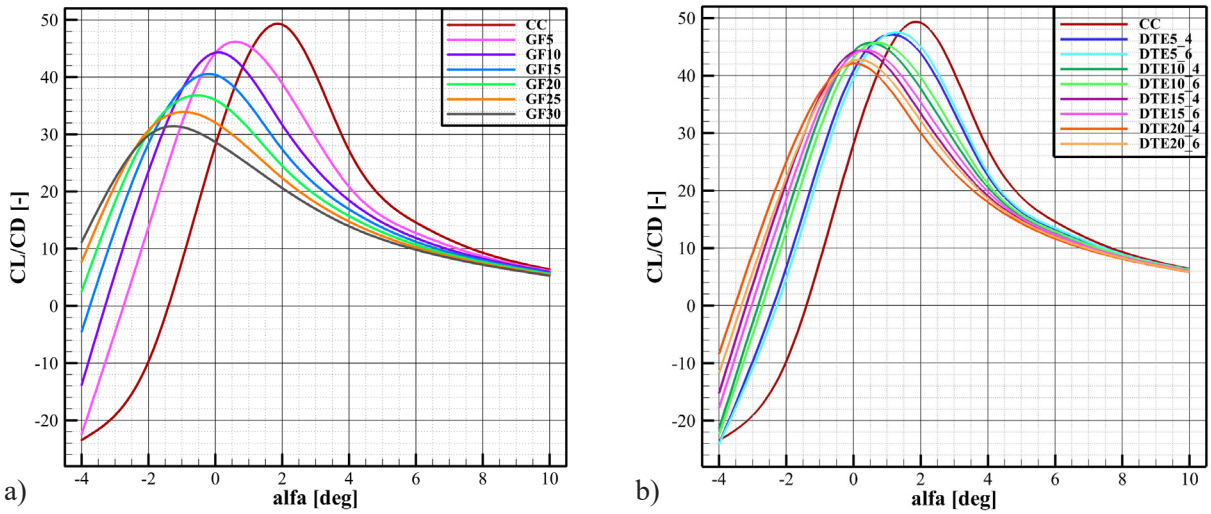

Fig. 9. Comparison of lift-to-drag ratio versus alpha of RAE-2822 airfoil (a) with/without GF, (b) with/without DTE

Based on the data shown in Figures 8 and 9, the flap variants achieved the highest aerodynamic efficiency values at smaller angles of attack compared to the clean profile. As the flap size increased, the maximum aerodynamic efficiency value decreased and was achieved at progressively smaller angles of attack. For angles of attack below -2°, the Gurney flap maintained higher aerodynamic efficiency values than the Divergent Trailing-edge flap. Beyond 8°, the applied modifications had little impact on the achieved aerodynamic efficiency values, with all curves converging closely.

Figures 9 and 10 illustrate the dependencies of the lift-drag ratio on the angle of attack and the lift coefficient, respectively. In scenarios where generating high lift is unnecessary, the clean profile achieves a better lift-drag ratio. However, when additional lift is required on the wing, the GF flap profile achieves higher values than the DTE flap profile. The developed simulation model aimed at investigating the effects of variations in Gurney flaps and Divergent Trailing-edge flaps on the aerodynamics of the RAE-2822 profile across different angles of attack has yielded pivotal findings and conclusions, as discussed in this scientific article. Both GF and DTE flaps proved to be highly effective in increasing the lift coefficient compared to the clean profile, a crucial advantage for aircraft performance, particularly during take-off and

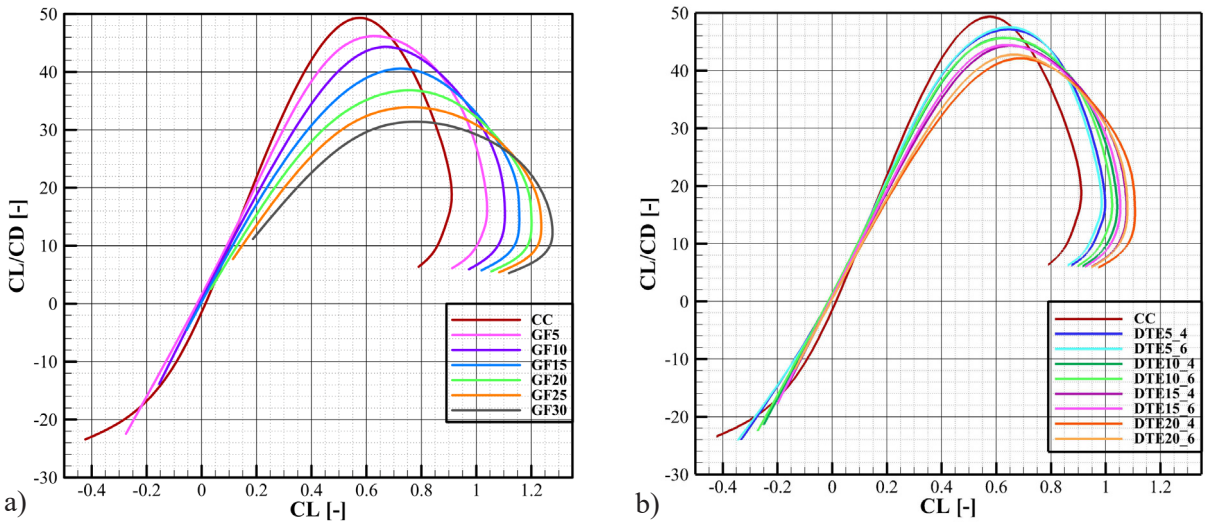

Fig. 10. Comparison of lift-to-drag ratio versus lift coefficients of RAE-2822 airfoil (a) with/without GF, (b) with/without DTE.

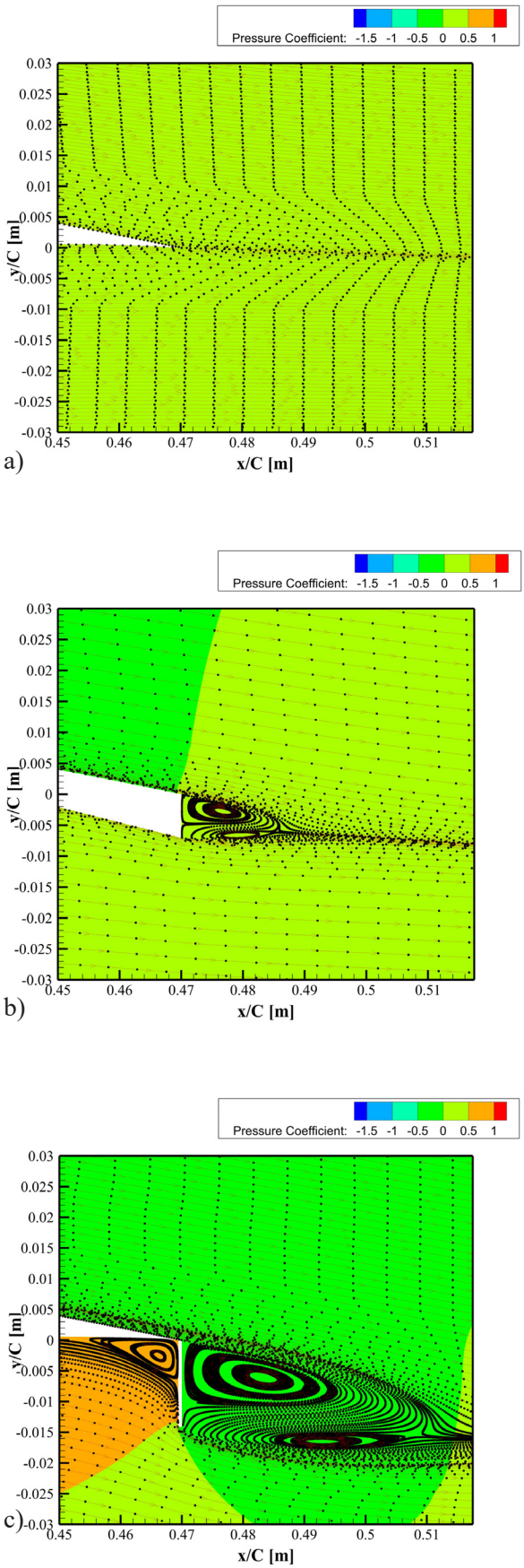

Fig. 11. Flow structure and pressure contours on the Trailing-edge of RAE-2822 airfoil a) clean airfoil, b) with DTE 15_4, c) with GF 30 at alpha=0°

landing. Moreover, within the range of angles of attack from -4 to 0 degrees, both types of trailing-edge modifications demonstrated improved aerodynamic efficiency, striking a favorable balance between lift and drag for enhanced fuel efficiency and range. These modifications also contributed to augmenting payload capacity, with Gurney flaps offering superior lifting force and size reduction capabilities, particularly advantageous for compact aircraft like drones. Additionally, Trailing-edge modifications held promise for shortening take-off and landing distances, which could be beneficial in diverse operational scenarios. As technology evolves, transonic drones may see increased utilization, further underscoring the potential importance of Trailing-edge modifications in advancing their performance and efficiency.

Notably, Gurney flaps exhibited distinct advantages, boasting superior lift coefficients compared to DTE flaps of similar size. They excelled in increasing payload capacity and reducing aircraft size. On the other hand, DTE flaps showcased their strength in projects aiming for heightened aerodynamic efficiency and range, fostering economical operation and extended aircraft range through lower drag coefficients and enhanced overall efficiency. This study underscores the importance of selecting the appropriate flap type based on specific aircraft design objectives, offering valuable design flexibility. However, certain limitations and considerations emerged from this research. Range and economical operation may not be paramount for small drones, often operating within short distances, potentially diminishing the pronounced benefits of Trailing-edge modifications in such cases. Furthermore, while informative, the study calls for further research to deepen our understanding and optimize the application of these Trailing-edge modifications, hinting at untapped potential and unexplored limitations.

Influence of flap applications on fluid flow structure

To show the impact of the use of the Gurney flap and the Divergent Trailing-edge flap on the image of the flow structure, streamlines were generated for profiles with flaps and a clean profile for M=0.73 and alpha=0°. The streamline and pressure distribution are shown in Figure 11 for a clean airfoil with a GF flap and a DTE 15_4 flap. There is no flow separation at the Trailing-edge for a clean airfoil. In the case of an airfoil with a flap, the boundary layer

is torn off, vortices are formed behind the Trailing-edge, and the vortex area for the airfoil with a flap GF is longer than the area of vortices in front of the flap GF (on the overpressure side), which does not occur for the airfoil with a flap DTE. It can be observed that the streams of fluid flowing down the profile due to the action of the vortices are deflected downwards, which directly translates into an increase in the lift force, according to the characteristics presented in Figures 6-10.

CONCLUSIONS

In this research, we conducted numerical simulations of transonic flow to investigate how variations in the dimensions of the Gurney flap and the Divergent Trailing-edge flap influence the aerodynamics of the RAE-2822 profile across different angles of attack. For both flap types and across all angles of attack tested, we observed an increase in the lift coefficient (C_L) compared to the clean profile. Additionally, an increase in the drag coefficient (C_D) was noted for angles exceeding approximately -3 degrees, with the magnitude of this increase dependent on the flap height relative to the clean profile.

In the range of angles of attack from -4 to 0 degrees, both Trailing-edge modifications resulted in higher aerodynamic efficiency values. For instance, consider the GF_1.5 flap at an angle of attack of -1.5 degrees, where the achieved lift coefficient was approximately 0.45, representing typical cruising conditions. At the same angle, the aerodynamic lift-to-drag achieved with this flap surpassed the clean profile. Trailing-edge modifications are pivotal in augmenting an aircraft's lift force. Furthermore, when comparing GF flaps to DTE flaps of the same size (flap height), GF flaps exhibited superior lift coefficients. For the design goal of minimizing aircraft size, especially in the case of drones, GF flaps are superior to DTE flaps, allowing a more significant reduction in aircraft size. The additional lift generated by the GF flap compensates for the decrease in lift due to the reduction in aircraft size resulting from the design requirements.

Both flaps contribute to increasing the payload capacity of the aircraft. Still, due to the greater lifting force generated, the GF flap allows a more efficient increase in the payload carried than the DTE flap. For the above two design goals, GF flaps of 0.5% to 2% of the chord length would be a good option, as they increase the lift coefficient while minimally increasing the drag coefficient. The DTE flap is a better solution for projects that aim to provide greater aerodynamic efficiency and range, as it leads to more economical operation and greater aircraft range due to the lower drag coefficients and better efficiency achieved. On the other hand, if the goal is to provide greater aerodynamic efficiency and range while reducing the drone's size or increasing its payload, DTE flaps are a better solution. However, it is worth noting that range and economical operation are not always crucial criteria for small drones, which often operate at short distances. In such applications, GF flaps usually better meet the design requirements.

The need for Trailing-edge modifications is always based on the design of the aircraft. Using a Gurney flap does not always positively affect the range of the aircraft, but it may bring other benefits. UAVs (Unmanned Aerial Vehicles) are a specific group of aircraft whose design assumptions are often more rigorous. Unmanned aerial vehicles accelerating to transonic speeds are mainly used in military technology due to their increased safety during military operations. Drones used for research or scientific purposes do not need to develop transonic speeds for economic reasons. However, it is expected that with the development of technology, the use of transonic drones will become more common. Using the considered Trailing-edge modifications may translate into an increase in the carried load and a reduction in the drone's size by reducing the required wingspan. It may also shorten the required take-off and landing distance.

Conclusions from the study indicate that Trailing-edge modifications, especially GF flaps, can be a crucial element in designing effective and efficient aircraft, especially for small drones where payload and size are essential. However, further research is recommended to understand and optimize these solutions. In further research, it would be worth considering the effect of mini TEDs at low Reynolds numbers, which would allow assessing their impact during take-off and landing. Conclusion underscores the potential of combining mini Gurney flaps and Vortex Generators as passive flow control devices to enhance the aerodynamic performance of airfoils and wind turbine rotor blades with implications for improving the efficiency and power generation. In further research, it would be worth considering the introduction of Vortex Generators in combination with mini TEDs in drone applications.

REFERENCES

1. Didwania M., Khatri K.K. Analysis of Stalling Over FLAPED Wing of an Aeroplane by CFD Code Analysis of Stalling Over FLAPED Wing of an Aeroplane by CFD Code 2021; May. doi: 10.9790/1684-1604044554.
2. Ko S., Bae J., Abdelrahman A., Wang L. Aerodynamic performance analysis of a trailing- edge flap for wind turbines Aerodynamic performance analysis of a trailing-edge flap for wind turbines.
3. Bechert D.W., Meyer R., Hage W., Drag reduction on gurney flaps and divergent trailing edges, 2001; 229–245.
4. Gopalakrishnan Meena M., Taira K., Asai K. Airfoil-Wake Modification with Gurney Flap at Low Reynolds Number. AIAA Journal, 2018; 56(4): 1348–1359. doi: 10.2514/1.J056260.
5. Cole J.A., Vieira B.A.O., Coder J.G., Premi A., Maughmer M.D. Experimental investigation into the effect of gurney flaps on various airfoils. Journal of Aircraft, 2013; 50(4), 1287–1294. doi: 10.2514/1.C032203.
6. Wang J.J., Li Y.C., Choi K.-S. Gurney flap – Lift enhancement, mechanisms and applications . Progress in Aerospace Sciences, 2008; 44(1): 22–47. doi: 10.1016/j.paerosci.2007.10.001.
7. Alber J., et al., Experimental investigation of mini Gurney flaps in combination with vortex generators for improved wind turbine blade performance, 2022; 943–965.
8. Singh D.A.I., Effect of Gurney flap on the vortex - dominated flow over low - AR wings, 2023.
9. Liebeck R.H., Design of subsonic airfoils for high lift. Journal of Aircraft, 1978; 15(9): 547–561. doi: 10.2514/3.58406.
10. Poole D.J., Allen C.B., Rendall T.C.S., Comparison of point design and range-based objectives for transonic aerofoil optimization. AIAA Journal, 2018; 56(8), 3240–3256. doi: 10.2514/1.J056627.
11. Yu T., Wang J.J., and Zhang P.F., Numerical simulation of gurney flap on RAE-2822 supercritical airfoil, Journal of Aircraft, 2011; 48(5), 1565–1575, doi: 10.2514/1.C031285.
12. Thompson B.E., Lotz R.D., Divergent-trailing-edge airfoil flow. Journal of Aircraft, 1996; 33(5), 950–955. doi: 10.2514/3.47040.
13. Yu T., Wang J.J., Zhang P.F. Numerical Simulation of Gurney Flap on RAE-2822 Supercritical Airfoil. Journal of Aircraft, 2011; 48(5): 1565–1575. doi: 10.2514/1.C031285.
14. Chandrasekhara M.S., Optimum Gurney flap height determination for 'lost-lift' recovery in compressible dynamic stall control. Aerospace Science and Technology, 2010; 14(8), 551–556. doi: 10.1016/j.ast.2010.04.010.
15. Maughmer M.D., Bramesfeld G. Experimental Investigation of Gurney Flaps. Journal of Aircraft, 2008; 45(6), 2062–2067. doi: 10.2514/1.37050.
16. Giguere P., Lemay J., Dumas G. Gurney flap effects and scaling for low-speed airfoils, Jun., 1995. doi: 10.2514/6.1995-1881.
17. Li Y., Wang J., Zhang P. Influences of Mounting Angles and Locations on the Effects of Gurney Flaps. Journal of Aircraft, 2003; 40(3), 494–498. doi: 10.2514/2.3144.
18. Richter K., Rosemann H. Steady Aerodynamics of Miniature Trailing-Edge Devices in Transonic Flows, Jun., 2011. doi: 10.2514/6.2011-3354.
19. Akdeniz H.Y. International Journal of Aviation A Study on Aerodynamic Behavior of Subsonic UAVs ' Wing Sections with Flaps, 2021; 2(1), 22–27. doi: 10.23890/IJAST.vm02is01.0103.
20. Speeds T. Aerodynamic Loads Alteration by Gurney Flap on Supercritical Airfoils at Aerodynamic Loads Alteration by Gurney Flap on Supercritical Airfoils at Transonic Speeds no. September 2018, 2019.
21. Yoo Y. Aerodynamic Performance Improvement by Divergent Trailing Edge Modification to a Supercritical Airfoil + M, 2001; 15(10): 1434–1441.
22. Makgantai B., A Review on Wingtip Devices for Reducing Induced Drag on Fixed-Wing Drones, 13(11): 143–160.
23. Hassanalian M., Abdelkefi A. Classifications, applications, and design challenges of drones: A review, Progress in Aerospace Sciences, 2017; 91(May): 99–131. doi: 10.1016/j.paerosci.2017.04.003.
24. Valavanis G.J., Vachtsevanos K. Handbook of Unmanned Aerial Vehicles. Springer Netherlands, 2015.
25. Winiarski P., Pods S., Szwedziak K., Łusiak T., Robert B. Wind Tunnel Experiments on an Aircraft Model Fabricated Using a 3D Printing Technique, 2022.
26. Setlak L., Kowalik R., Practical Use of Composite Materials Used in Military Aircraft 2021.
27. Hirsch C., Numerical Computation of Internal and External Flows, Volume 2: Computational Methods for Inviscid and Viscous Flows. John Wiley & Sons, Inc., 1991.
28. Wilcox D.C Turbulence Modeling for CFD, Third Edft. Canada, CA, USA: DCW Industries, 2006.
29. He X. et al., Numerical Simulation of Gurney Flap on SFYT15thick Airfoil, 2016. doi: 10.1016/j.taml.2016.09.002.
30. M.A.M. and M.C.P.F.P.H. Cook Aerofoil Rae 2822: Pressure Distributions, and Boundary Layer and Wake Measurements, Experimental Data Base for Computer Program Assessment, AGARD Report ar 138, 1979.
31. Coakley T. Numerical simulation of viscous transonic airfoil flows, Mar. 1987, doi: 10.2514/6.1987-416.